GaN-based Tunnel Junction in Optical Devices

T. Takeuchi[a], G. Hasnain[a], S. Corzine[a], M. Hueschen[a], R.P. Schneider, Jr.[a], C. Kocot[a], M. Blomquvist[a], Y.-L. Chang[a], D. Lefforge[a], M. R. Krames[b], L.W. Cook[b], S.A. Stockman[b], J. Han[c], M. Diagne[d], Y. He[d], E. Makarona[d], A. Nurmikko[d]

[a]Agilent Technologies Laboratories, 3500 Deer Creek Road, Palo Alto, CA 94304
[b]Lumileds lighting, 370 West Trimble Road, San Jose, CA 95131
[c]Department of Electrical Engineering, Yale University, New Haven, CT
[d]Division of Engineering and Department of Phsics, Brown University, Providence, Rhode Island 02912

ABSTRACT

We have demonstrated hole injection through a tunnel junction embedded in the GaN-based light emitting diode structure. The tunnel junction consists of 30 nm GaN:Si^{++} and 15 nm InGaN:Mg^{++} grown on a GaN-InGaN quantum well heterostructure. The forward voltage of the light emitting diode, including the voltage drop across the reverse-biased tunnel junction, is 4.1 V at 50 A/cm^2, while that of a standard light emitting diode with a conventional contact structure is 3.5 V. The light output of the diode with the tunnel junction is comparable to that of the standard device. We then employed the tunnel junction in vertical cavity surface emitting laser structures and dual-wavelength light emitters. In the vertical cavity structure, a good lateral current spreading was accomplished, resulting in uniform emission pattern. The dual-wavelength light emitter has been operated as a three-terminal device with independent electrical control of each LEDs to a nsec time scale.

1. INTRODUCTION

AlGaInN is one of the most promising material systems for short wavelength optoelectronic devices and high power electronic devices because of its wide direct bandgap. Blue and green InGaN light emitting diodes (LEDs),[1] including high-power LEDs,[2] and near-ultraviolet laser diodes[3-5] have been demonstrated and are now commercially available. In addition, optically-pumped vertical cavity surface emitting lasers have been demonstrated.[6,7]

One of the remaining issues in GaN-based material research is the low hole concentration and the high resistivity of p-type layers.[8,9] InGaN layers with very high carrier concentrations (p~1×10^{19} cm^{-3} at 300K) have been demonstrated,[10] but the resistivity of p-GaN is typically 100 times higher than that of n-GaN, resulting in poor lateral current spreading within p-GaN layers. For instance, to achieve reasonable current spreading and light extraction simultaneously in a top-emitting LED structure, a semi-transparent (semi-absorbing) p-type electrode is typically employed. However, this approach leads to a trade-off between forward voltage and light extraction efficiency, which both depend sensitively on the electrode thickness. Instead, a substrate-emitting LED, employing a flip-chip structure, could evade this issue because light emission is extracted from the other side of the electrode, which can be made thick and reflective.[2] However, the flip-chip structure normally requires a separate submount carrier or special package for electrical interconnection, which adds cost and manufacturing complexity, especially for smaller-area chips. Additionally it is very difficult to obtain low resistivity p-AlGaN, especially with more than 10% AlN molar fraction,[11] limiting the realization of shorter wavelength laser diodes as well as GaN-based vertical cavity surface emitting lasers (VCSELs).

Recently hole injection through a reverse-biased tunnel junction has been used to provide low-resistance lateral current flow in InGaAs VCSELs and resonant-cavity LEDs employing oxide-based ditributed Bragg reflectors.[12] This technique has been similarly employed to minimize the portion of p-type material in an InP-based VCSEL[13,14] since the InP-based p-layer has relatively high resistivity, leading to serious heating problems. The hole injection through the tunnel junction is also conceivable in GaN-based material for alleviating problems related to the highly resistive p-layers. Recently S.-R.

Jeon et al. demonstrated a lateral current spreading at the top n-GaN layer in the LED structure with a GaN tunnel junction.[15]

In this paper, we demonstrate hole injection through a GaN:Si^{++}/InGaN:Mg^{++} tunnel junction in the LED structure, showing reasonably low voltage drop at the tunnel junction and no observed penalty for light output intensity.[20] We also employ this tunnel junction in VCSEL structures[21] and dual-wavelength light emitters,[22] leading to significant improvements of the device performances.

2. EXPERIMENTS

All the samples here were grown on sapphire (0001) substrates with low-temperature-deposited buffer (LT-buffer) layer[16] by low-pressure metalorganic chemical vapor deposition. TMGa, TEGa, TMAl, and TMIn were used as group-III sources, and NH_3 was used as a group-V source. Cp_2Mg and SiH_4 were used as dopant precursors for p-type and n-type, respectively. InN and AlN mole fractions in layers were determined from X-ray diffraction patterns assuming that the layers are fully relaxed in this experiment. Hall effect measurements were performed to determine hole carrier concentrations after thermal annealing at 700 °C for 5 min.[9] Mg and Si concentrations in the layers were determined by secondary ion mass spectrometry (SIMS) analysis.

3. RESULTS AND DISCUSSION

3.1 Mg-doped InGaN, GaN, and AlGaN

Generally very high carrier/doping concentrations are required to obtain lower voltage drop across the reverse-biased tunnel junction,. We first investigated the electrical properties of our Mg-doped InGaN, GaN, and AlGaN. The sample structure for Hall effect measurements consists of a 30 nm GaN LT-buffer layer, a 3 μm undoped GaN, and a 0.4-0.6 μm Mg-doped InGaN, GaN, or AlGaN. Mg concentrations of all the samples are 1-5 x 10^{19} cm^{-3}, confirmed by SIMS. Figure 1 shows hole carrier concentration at room temperature as a function of InN or AlN mole fraction. The hole carrier concentration was increased as the bandgap was narrower, that is, less AlN and more InN mole fraction. The highest hole carrier concentration, 1.9 x 10^{18} cm^{-3}, was obtained with $In_{0.18}Ga_{0.82}N$ in this experiment, while the hole carrier concentration of GaN was 3.9 x 10^{17}cm^{-3}. On the other hand, the hole carrier concentration of AlGaN was very low, 4.0 x 10^{16} cm^{-3}, with 14 % AlN mole fraction. This clearly explains the difficulty of the realization of the shorter wavelength lasers and VCSELs both require the AlGaN layers with high (over 10 %) AlN mole fraction. As a result, we concluded that InGaN is more suitable material than GaN as the p-layer in tunnel junctions.

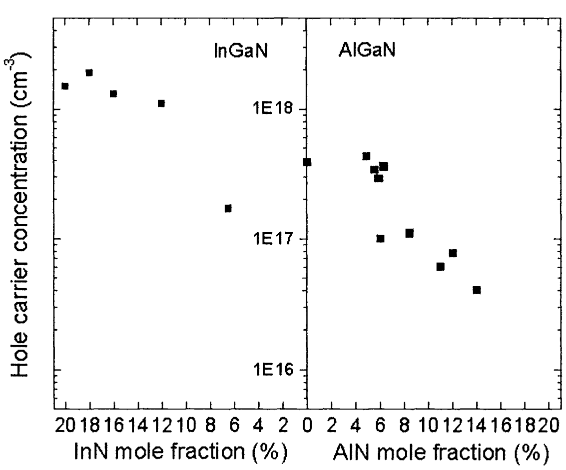

Fig. 1 Hole carrier concentration at room temperature as a function of InN or AlN mole fraction.

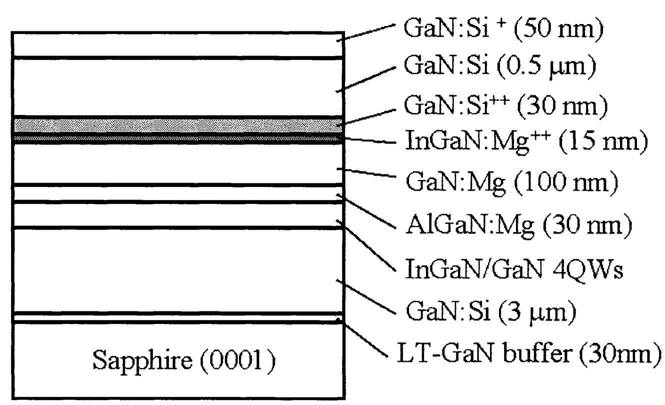

Fig. 2 Schematic of GaN-based LED structure with the tunnel junction.

3.2 InGaN/GaN tunnel junction

Figure 2 shows the LED structure with the tunnel junction, consisting of a 30 nm GaN LT-buffer layer, a 3 μm bottom n-GaN layer, four InGaN quantum wells with GaN barriers, a 30 nm p-AlGaN layer, a 100 nm p-GaN layer, a 15 nm InGaN:Mg^{++} layer, a 30 nm GaN:Si^{++} layer, a 0.5 μm top n-GaN layer and a 50 nm n^+-GaN contact layer. The InN mole fraction in the tunnel junction layer is kept lower than that in the quantum wells to prevent optical absorption of emission from the wells. We prepared four LED structures with tunnel junctions having different doping levels. We also prepared a standard LED structure for comparison, which has a p^+-GaN contact layer on the top of the 100 nm p-GaN layer, instead of the tunnel junction and the top n-GaN layer. After finishing the growth, we then removed the upper layers by dry etching to expose the bottom n-GaN layer for the bottom n-contact. The diameter of the top n-contact was 100 μm. We measured the light output intensity from the substrate side using a Si photodetector under DC bias at room temperature. The peak emission wavelength of all the samples was around 480nm.

As shown in Figure 3, the highest doping concentrations, approximately 2 x 10^{20} cm^{-3} Mg and 3 x 10^{20} cm^{-3} Si, were achieved, while we found that a Mg memory effect resulted in a large amount of Mg (~ 1 x 10^{18} cm^{-3}) incorporating into the following Si-doped GaN layers. Table 1 shows the various doping concentration levels of Mg and Si at tunnel junctions in four LED structures and their forward voltages at current density of 50 A/cm^2. We found that very high doping concentrations (over 2 x 10^{20} cm^{-3}) for both n- and p-layers are crucial to achieve a lower resistance of the reverse-biased tunnel junction.

Figure 4 shows the comparison of voltage vs. current density characteristics between the LEDs with tunnel junctions and the standard LED with the conventional p-contact. Our standard LED with the semi-transparent current-spreading contact exhibited a forward voltage of 3.5 V at 50 A/cm^2. This value is similar to previous reports.[1,2] The LED with the lowest doping levels at the tunnel junction (sample A) showed very high forward voltage, 6.7 V at 50 A/cm^2. On the other hand, the forward voltage of the LED with the highest doping levels at the tunnel junction (sample D) was reasonably low, 4.1 V. We conclude that the voltage drop at the tunnel junction with the highest doping levels is about 0.6 V at 50 A/cm^2, subtracting the forward voltage of our standard LED from that of the LED with the tunnel junction. This value is still very high compared to the values of InP-based[13,14] and GaAs-based tunnel junctions.[17-19] This could be due to a large bandgap as well as the difficulty in achieving a sufficiently high acceptor and hole concentrations in GaN-based materials.

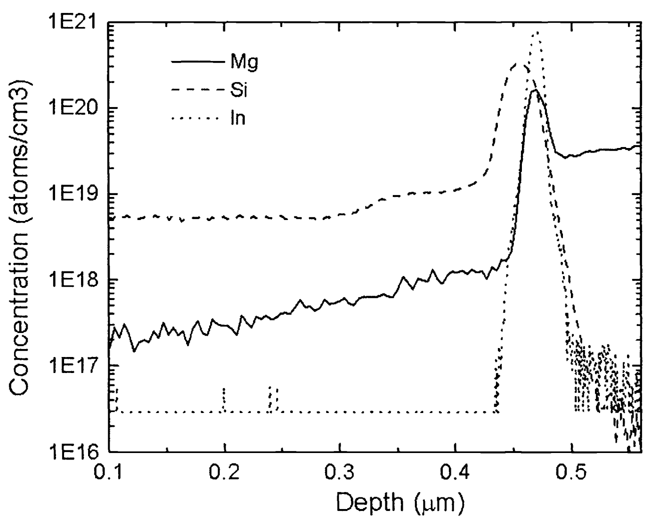

Fig. 3 SIMS profile of the portion of the tunnel junction with the highest doping levels.

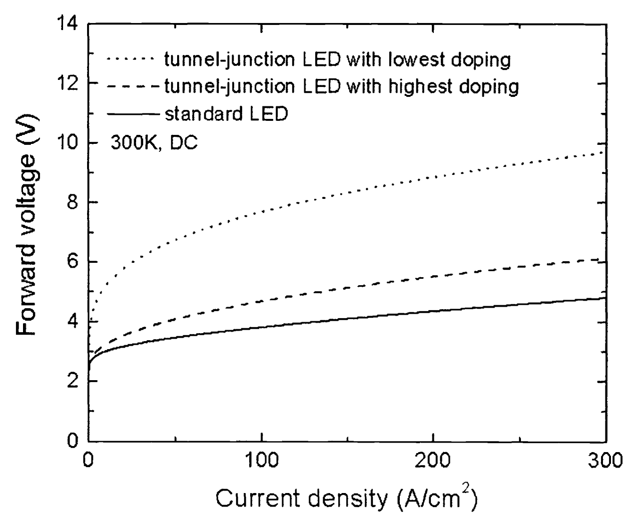

Fig. 4 Voltage vs. current density characteristics of the LED with the lowest doping concentrations at the tunnel junction, the LED with the highest doping concentrations, and the standard LED with p-contact.

Table 1 doping concentrations of Si and Mg at tunnel junctions and forward voltages at current density of 50 A/cm^2.

	Si in GaN (x 10^{20} cm^{-3})	Mg in InGaN (x 10^{20} cm^{-3})	Voltage at 50 A/cm^2 (V)
sample A	0.6	1	6.7
sample B	1	1	4.9
sample C	3	1	4.5
sample D	3	2	4.1

Figure 5 shows light output vs. current density characteristics for the LED with the tunnel junction (the highest doping levels), and for the standard LED. Note that light output was measured through the sapphire substrate. No light output penalty was observed by inserting the heavily doped tunnel junction on the top of the quantum wells with the 100 nm p-GaN spacer layer, indicating that the hole injection through the tunnel junction is sufficient and the optical quality of the active region remains high. Therefore, assuming that the current spread at the top n-GaN layer is sufficient,[15] one can estimate that the light extraction efficiency of the top-emitting LED with tunnel junction could compare to that of a flip-chip LED, which for large-area (~ 1 x 1 mm^2) devices is 1.6 times higher than that of the standard top-emitting LED with semi-transparent p-contact.[2]

3.3 Vertical cavity surface emitting laser structure

Figure 6 shows a VCSEL structure with the tunnel junction as well as the crack-free GaN/AlGaN distributed Bragg reflector (DBR). Following the growth of a GaN layer using LT-buffer, a 60 pair GaN/$Al_{0.25}Ga_{0.75}N$ DBR was grown using AlN strain relief layers.[23, 24] This AlN layer greatly reduces the number of cracks even in such a thick (~5 μm) GaN/AlGaN heterostructures so that crack-free region was obtained over several cm^2. A peak reflectivity of 0.99 was obtained with approximately 15nm spectral bandwidth. The active region consists of $In_{0.08}Ga_{0.92}N$/GaN 7QWs designed for the emission at 410 nm, surrounded by 100 nm AlGaN cladding layers. Then the 15nm InGaN:Mg^{++}/30nm GaN:Si^{++} tunnel junction and a 200 nm n-GaN layer were grown to obtain an intracavity lateral current spreading. The InN mole

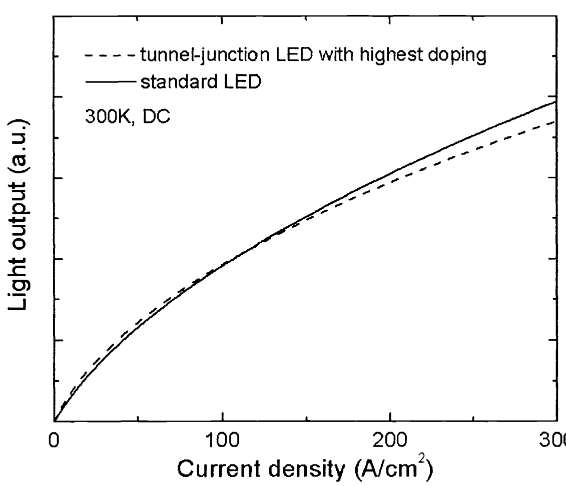

Fig. 5 Light output vs. current density characteristics of the LED with the highest doping concentrations at the tunnel junction compared to the standard LED with p-contact. Note that light output was measured through the sapphire substrate.

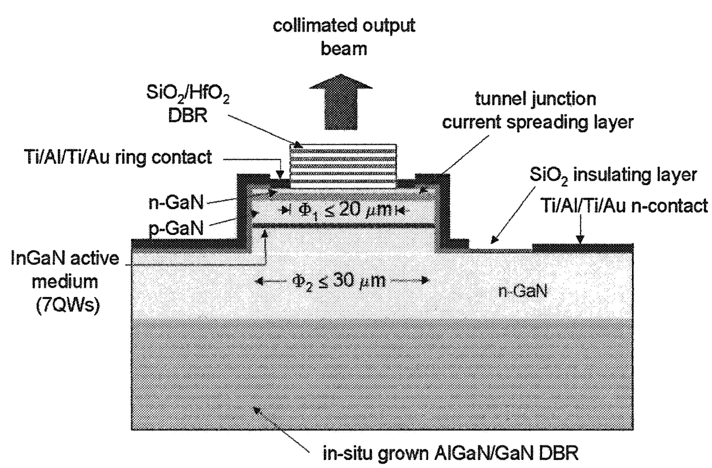

Fig. 6 Schematic of the VCSEL structure with the tunnel junction as well as GaN/AlGaN DBR.

fraction in the tunnel junction is slightly lower than that of the active region InGaN. The doping concentrations in the tunnel junctions are the same as those in the LED structures described in section 3.2. Finally the vertical cavity was completed with a dielectric SiO_2/HfO_2 DBR deposited by reactive ion beam sputtering. The top dielectric DBR was patterned so that the device had an effective optical aperture varying from 10 to 30 μm. Standard lithographic and dry etching techniques were used to provide the electric contacts, in form of a Ti/Al/Ti/Au annular ring to the top n-GaN and a deep etched contact area for the bottom n-GaN. The deep etch step defined the diameter of the mesa in Figure 6 in the range of 20 to 50 μm.

Figure 7 shows the current density vs. voltage characteristics of a typical device, at two levels of continuous injection at room temperature. In the low injection regime, characteristic of a LED (~100 A/cm^2), the presence of the tunnel junction typically added up to 1 V to the forward voltage characteristics, which is consistent with the previous LED result as shown in Fig.4. At higher injection levels (~1 kA/cm^2), we saw evidence of additional series resistance, assigned in part to the presence of the tunnel junction. Nonetheless, the lateral current spreading was clearly accomplished so that the light emission from the devices was uniform in its average intensity across the emitting aperture, as illustrated in the photograph in the inset of Fig. 8. However, when examining the emission under high spatial resolution (~1 μm) we have found evidence of some tendency towards "filamental" vertical conduction, reflective perhaps of the influence of local compositional or doping inhomogeneities within the tunnel junction.

Figure 8 shows the output spectrum of a typical device at operating current density of 0.2 kA/cm^2. The emission was observed in the direction normal to the planar device, with apertures and imaging optics restricting the angular view to approximately 10 degrees. While the cavity is rather thick (over 10 λ), only two vertical cavity modes are seen, indicating the restrictively narrow spectral bandwidth of the GaN/AlGaN DBR. The dominant mode at 413 nm has a spectral linewidth of approximately 0.6 nm. This value is comparable to the linewidth previously measured in our best structures that were designed for optically pumped VCSEL operation.[7]

3.4 Dual-wavelength light emitter

Figure 9 shows a novel GaN-based LED configuration in which two electrically independent InGaN QWs of different indium composition are built into a single vertical heterostructure. The device incorporates the InGaN/GaN tunnel junction which separates the two active regions so that a three-terminal device can be implemented which permits the

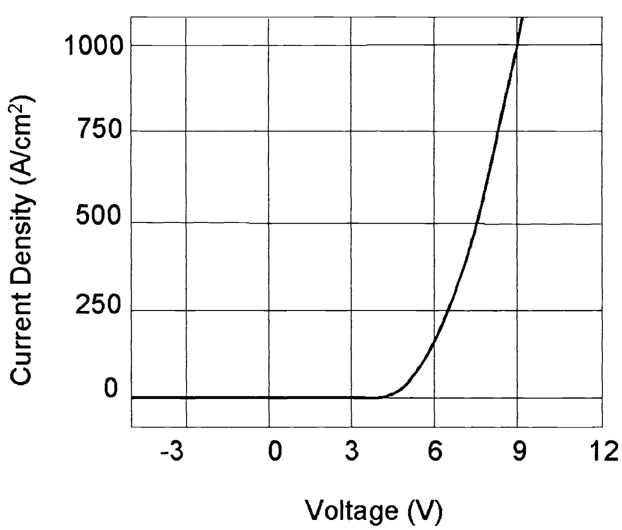

Fig. 7 Current density vs. voltage characteristics of a device with a 20 μm diameter mesa defining the vertical current path.

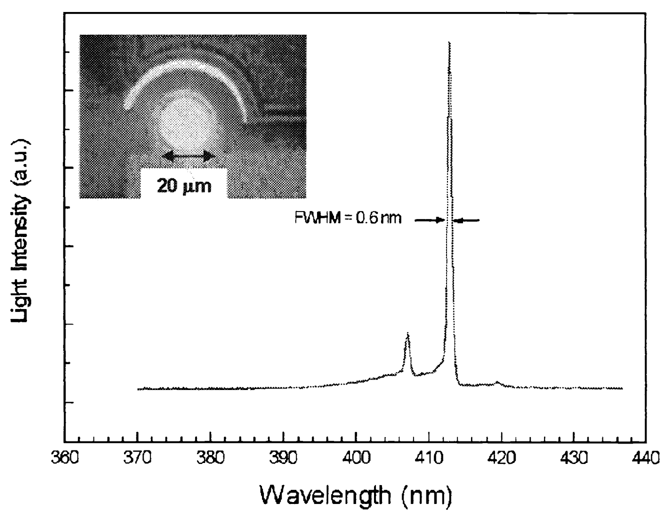

Fig. 8 Emission spectrum of a device at 0.2 kA/cm^2. The inset shows the plan view photograph of the device with emission filling an effective aperture of approximately 20 μm.

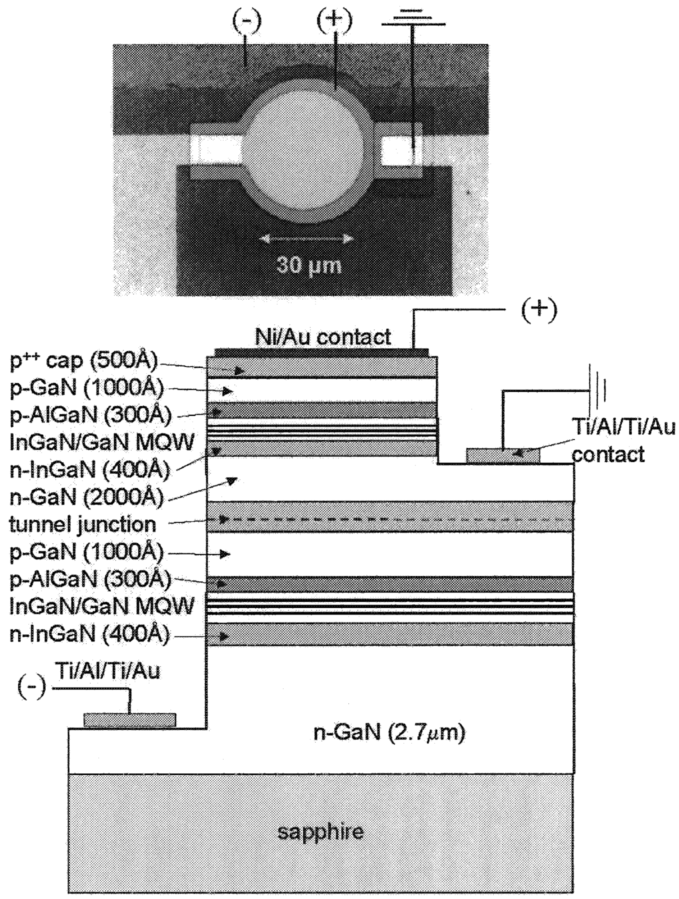

Fig. 9 Schematic view of the two-wavelength blue-green LED, indicating the active regions, the tunnel junction, and the bias arrangement. A plan view photograph of a device is shown at the top.

operation of the LEDs as a time-multiplexed two-color source. The bottom LED segment was grown on a n-GaN layer, with the active region composed of four InGaN/GaN QWs, designed for emission at 530 nm. The tunnel junction segment was grown on the top 100 nm p-GaN, consisting of 15 nm InGaN:Mg^{++}/30 nm GaN:Si^{++}. Then the top LED segment was grown on the tunnel junction with the top 200 nm n-GaN. The active region in the top LED composed four InGaN/GaN QWs with the composition aimed at emission wavelength of 470 nm. The structure was completed with a 50 nm heavily doped p-GaN cap layer for fabricating the Ni/Au electrical contact. The fabrication of the three-terminal device involved standard lithography and etching steps to define a circular emitter. Two etch steps were required, to reach the bottom LED's n-GaN layer and the common ground for the two LED segments, respectively. The diameter of the top and bottom LEDs are 60 and 80 µm, respectively. Note that we collected the emission through the sapphire substrate.

Figure 10 shows the current vs. voltage characteristics of the top and bottom LEDs. As similarly seen in section 3.3, the presence of the tunnel junction in the bottom devices typically added about 1V to the forward voltage characteristics, when compared with the top LED without the tunnel junction in the low injection regime (~100 A/cm^2). We also found the additional series resistance at the high injection level and the "filamental " vertical conduction under the high spatial resolution.

Spectral characteristics of the device structure are shown in Figure 11, where the light solid curve was obtained by turning each LED on by a separate pulsed bias supply in a time sequential manner, while the bold line was obtained by

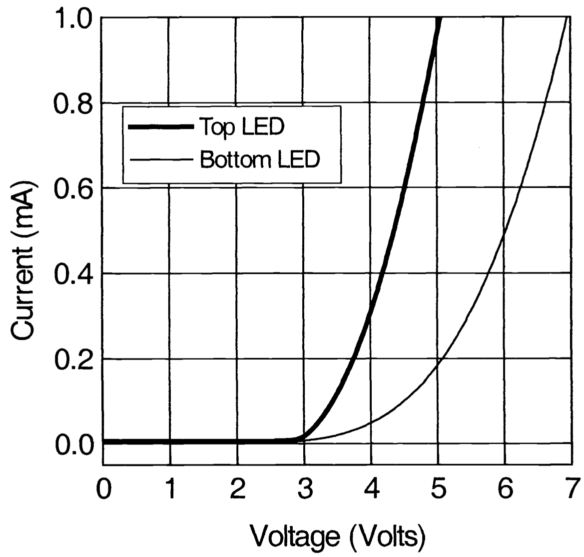

Fig. 10 Current vs. voltage characteristics of the top and bottom LEDs.

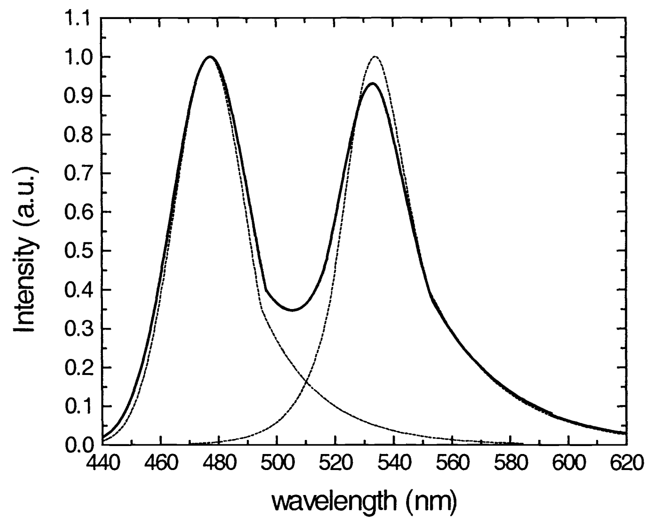

Fig. 11 Comparison of the emission spectra from the top and bottom LEDs when the LEDs are activated independently in a three-terminal case (light solid curve), and their simultaneous activation in the two-terminal case (bold curve).

operating the device as a simple two terminal device with a constant voltage applied across the top p-GaN and lowest n-GaN. Their electrical independence allowed us to program the 470 nm and 535 nm LEDs at any time sequence that we desired, up to speeds of nearly 100 MHz, without optimizing the impedance of terminal configuration. However, as the current voltage characteristics as well as their effective current apertures of the two LEDs were different, the applied voltage for each LED needed to be adjusted to obtain a comparable optical output from the devices.

4. CONCLUSION

We have demonstrated GaN-based tunnel junctions for hole injection in optical devices. The electrical properties of Mg-doped InGaN, GaN and AlGaN were investigated and the highest hole carrier concentration of 1.9 x $10^{18}cm^{-3}$ was achieved in $In_{0.18}Ga_{0.82}N$. By employing the InGaN:Mg^{++}/GaN:Si^{++} heterostructure with the very high doping concentrations, a reasonably low voltage drop (0.6 V at 50 A/cm^2) at the reverse-biased tunnel junction was obtained. There is no observed penalty in light output intensity by using the tunnel junction in the LED structure. The tunnel junctions were also utilized in the VCSEL structure and the dual-wavelength light emitters. In the vertical cavity structure, the good lateral current spreading was accomplished, resulting in the uniform emission pattern. The dual-wavelength light emitter has been operated as a three-terminal device with independent electrical control of each LEDs.

ACKNOWLEDGEMENTS

The authors are grateful to R. Twist, E. Liu, K. Than, and S. Song for their experimental support. The work at Brown University was supported by the National Science Foundation, the Defense Research Projects Agency, and by a grant from Lumileds Lighting LLC.

REFERENCES

1. S. Nakamura, M. Senoh, N. Iawsa, and S. Nagahama, “High-brightness InGaN blue, green and yellow light-emitting diodes with quantum well structures,” Jpn. J. Appl. Phys. **34**, L797 (1995).

2. J.J. Wierer, D.A. Steigerwald, M.R. Krames, J.J. O'Shea, M.J. Ludowise, G. Christenson, Y.-C. Shen, C. Lowery, P.S.Martin, S. Subaramanya, W. Goetz, N.F. Gardner, R.S. Kern, and S.A. Stockman, "High-power AlGaInN flip-chip light-emitting diodes," Appl. Phys. Lett. **78**, 3379 (2001).
3. I. Akasaki, S. Sota, H. Sakai, T. Tanaka, M. Koike, and H. Amano, "Shortest wavelength semiconductor laser diode," Electron. Lett. **32**, 1105 (1996).
4. S. Nakamura, M. Senoh, S. Nagahama, N. Iwasa, T. Yamada, T. Matsushita, H. Kiyoku, and Y. Sugimoto, "InGaN-based multi-quantum-well-structure laser diodes," Jpn. J. Appl. Phys. **35** L74 (1996).
5. G. Hasnain, T. Takeuchi, R. Schneider, S. Song, R. Twist, M. Blomqvist, C. Kocot, and C. Flory, "On-wafer continuous-wave operation of InGaN/GaN violet laser diodes," Electron. Lett., **36**, 1779 (2000).
6. T. Someya, R. Werner, A. Forchel, M. Catalano, R. Cingolani, and Y. Arakawa, "Room temperature lasing at blue wavelengths in gallium nitride microcavities," Science **285**, 1905 (1999).
7. Y.-K. Song, H. Zhou, M. Diagne, A,V, Nurmikko, R.P. Schneider, Jr., C.P. Kuo, M.R. Krames, R.S. Kern, C. Carter-Comam, and F.A. Kish, "A quasicontinuous wave, optically pumped violet vertical cavity surface emitting laser," Appl. Phys. Lett. **76**, 1662 (2000).
8. H. Amano, M. Kito, K. Hiramatsu, and I. Akasaki, "P-type conduction in Mg-doped GaN treated with low-energy electron beam irradiation (LEEBI)," Jpn. J. Appl. Phys. **28**, L2112 (1989).
9. S. Nakamura, M. Senoh, and T. Mukai, "Highly P-typed Mg-doped GaN films grown with GaN buffer layers," Jpn. J. Appl. Phys., **30**, L1708 (1991).
10. K. Kumakura, T. Makimoto, and N. Kobayashi, "Activation energy and electrical activity of Mg in Mg-doped $In_xGa_{1-x}N$ (x<0.2)," Jpn. J. Appl. Phys. **39**, L337 (2000).
11. M. Katsuragawa, S. Sota, M. Komori, C. Anbe, T. Takeuchi, H. Sakai, H. Amano, and I. Akasaki, "Thermal ionization energy of Si and Mg in AlGaN," J. Cryst. Growth, **189/190**, 528 (1998).
12. J.J. Wierer, D.A. Kellogg, and N. Holonyak, Jr., "Tunnel contact junction native-oxide aperture and mirror vertical-cavity surface-emitting lasers and resonant-cavity light-emitting diodes," Appl. Phys. Lett. **74**, 926 (1999).
13. S. Sekiguchi, T, Kimura, T. Miyamoto, F. Koyama, and K. Iga, "Long wavelength GaInAsP/InP laser with n-n contacts using AlAs/InP hole injecting tunnel junction," Jpn. J. Appl. Phys. **38**, L443 (1999).
14. M. Ortsiefer, R. Shau, G. Bohm, F. Kohler, G. Abstreiter, and M.-C. Amann, "Low-resistance InGa(Al)As tunnel junctions for long wavelength vertical-cavity surface-emitting lasers," Jpn. J. Appl. Phys. **39**, 1727 (2000).
15. S.-R. Jeon, Y.-H. Song, H.-J. Jang, G.M. Yang, S.W. Hwang, and S.J. Son, "Lateral current spreading in GaN-based light-emitting diodes utilizing tunnel contact junctions," Appl. Phys. Lett. **78**, 3265 (2001).
16. H. Amano, N. Sawaki, I. Akasaki, and T. Toyoda, "Metalorganic vapor phase epitaxial growth of a high quality GaN film using an AlN buffer layer," Appl. Phys. Lett. **48**, 353 (1986).
17. J.P. van der Ziel, W.T. Tsang, "Integrated multilayer GaAs lasers separated by tunnel junctions," Appl. Phys. Lett. **41**, 499 (1982).
18. A.R. Sugg, E.I. Chen, T.A. Richard, S.A. Maranowski, and N. Holonyak, Jr., "n-p-(p-n)-n $Al_yGa_{1-y}As$-GaAs-$In_xGa_{1-x}As$ quantum-well laser with p-n GaAs-InGaAs tunnel contact on n-GaAs," Appl. Phys. Lett. **62**, 2510 (1993).
19. J.Ch. Garcia, E. Rosencher, Ph. Collot, N. Laurent, J.L. Guyaux, J. Nagle, and E. Chirlias, "Epitaxially stacked GaAs/GaAlAs lasers using a low-resistance tunnel junction," J. Cryst. Growth **201/202**, 891 (1999).
20. T. Takeuchi, G. Hasnain, M. Hueschen, C. Kocot, M. Blomqvist, Y-.L. Chang, D. Lefforge and R. Schneider, M.R. Krames, L.W. Cook, and S.A. Stockman, "GaN-based light emitting diodes with tunnel junctions," Jpn. J. Appl. Phys. **40**, L861 (2001).
21. M. Diagne, Y. He, H. Zhou, E. Makarona, A.V. Nurmikko, J. Han, K. E. Waldrip, J. J. Figiel, T. Takeuchi, and M. Krames, "Vertical cavity viloet light emitting diode incorporationg an aluminum gallium nitride distributed Bragg mirror and a tunnel junction," Appl. Phys. Lett. **79**, 3720 (2001).
22. I. Ozden, E. Makarona, and A.V. Nurmikko, T. Takeuchi , and M. Krames, "A dual-wavelength indium gallium nitride quantum well light emitting diode," Appl. Phys. Lett. **79**, 2532 (2001).
23. K. E. Waldrip, J. Han, J. J. Figiel, H. Zhou, E. Makarona, and A.V. Nurmikko, "Stress engineering during metalorganic chemical vapor deposition of AlGaN/GaN distributed Bragg reflectors," Appl. Phys. Lett **78**, 3205 (2001)
24. H. Amano, M. Iwaya, N. Hayashi, T. Kashima, S. Nitta, C. Wetzel, I. Akasaki, "Control of dislocations and stress in AlGaN on sapphire using a low temperature interlayer," Phys. Status Solidi B, **216**, 683 (1999).